BIOCHEMISTRY
including biophysical chemistry & molecular biology

Article

pubs.acs.org/biochemistry

Polycystin-2 Induces a Conformational Change in Polycystin-1

Peter Oatley,[†] Md. Mesbah Uddin Talukder,[†] Andrew P. Stewart,[†] Richard Sandford,[‡] and J. Michael Edwardson*,[†]

[†]Department of Pharmacology, University of Cambridge, Tennis Court Road, Cambridge CB2 1PD, U.K.

[‡]Department of Medical Genetics, Cambridge Institute for Medical Research, Addenbrooke's Hospital, Cambridge CB2 0XY, U.K.

ABSTRACT: Autosomal dominant polycystic kidney disease (ADPKD) is caused by mutations in the genes encoding either polycystin-1 (PC1) or polycystin-2 (PC2). PC2 acts as a nonselective cation channel and together with PC1 plays a role in intracellular Ca^{2+} signaling. Using atomic force microscopy (AFM) imaging, we have shown previously that the N and C termini of PC1 appear as unequally sized particles connected by a "string" largely composed of tandem immunoglobulin-like, polycystic kidney disease (PKD) domains. Here, we show that coexpression of PC1 and PC2 causes an elongation of the PC1 string and a corresponding reduction in the size of the larger (C-terminal) particle. This change in the conformation of PC1 does not depend on its delivery to the plasma membrane. In addition, the use of the L3040H PC1 mutant showed that the conformational change does not require GPS cleavage. Coexpression of PC1 with PC2 mutants revealed that the conformational change in PC1 does not require either a stable interaction between PC1 and PC2 or PC2 channel function. Finally, we show that the tandem PKD repeats and to a lesser extent the receptor for egg jelly (REJ) domain both contribute to the extension of the PC1 string in the presence of PC2. We propose that the PKD repeats detach from the C-terminal fragment in response to PC2 activity. The resulting remodeling of PC1 may be responsible for enhancing GPS cleavage of PC1 and the separation of the PC1 N-terminal fragment from the C terminus during its maturation.

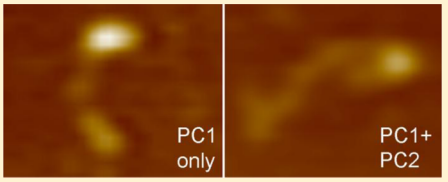

Autosomal dominant polycystic kidney disease (ADPKD) affects around one in a thousand individuals, making it one of the most common inherited diseases (reviewed in refs 1−3). Patients with ADPKD develop multiple fluid-filled cysts lined by renal tubular epithelial cells, which is a process that impairs kidney function and in many cases leads to end-stage renal failure. ADPKD is caused by mutations in either the *PKD1* or *PKD2* genes that encode the proteins polycystin-1 (PC1) and polycystin-2 (PC2), respectively.

PC2 is an ∼110 kDa multispanning transmembrane protein that belongs to the transient receptor potential (TRP) family and functions as a nonselective Ca^{2+}-permeable cation channel.[4,5] In addition to forming heterotetrameric complexes with other TRP channels, PC2 can form homotetramers.[6,7] PC2 homo-oligomerization is facilitated by domains at both the N and C termini,[8] and the oligomeric state of PC2 is modulated by Ca^{2+}-induced conformational changes in the EF-hand within its C-terminal cytoplasmic tail.[9]

PC1 is an ∼460 kDa integral membrane protein with 11 transmembrane domains and a large ∼3000 amino acid extracellular region containing several structural domains, including multiple immunoglobulin-like PKD repeats, a G-protein-coupled receptor proteolytic site (GPS), and a sea urchin receptor for egg jelly (REJ) domain (Figure 1). Atomic force microscopy (AFM) imaging of purified PC1 has revealed two unequally sized particles attached by a ∼35 nm string structure composed of tandem PKD repeats.[10] The vascular endothelial growth factor receptor-2, which also has several similar immunoglobulin-like repeats, has been shown by electron microscopy to adopt a similar structure.[11] Interestingly, epidermal growth factor receptor activation has been shown to enhance PC2 channel activity;[12] hence, these extended structures and the involvement of extracellular signals may be crucial for modulating PC2 function.

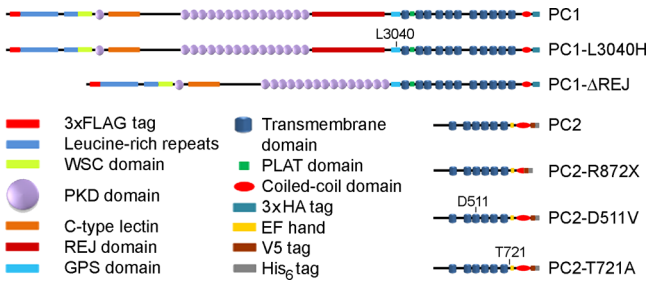

Figure 1. Schematic diagram of the PC1 and PC2 constructs. FL mouse PC1 contains a G protein-coupled receptor proteolytic site (GPS), tandem polycystic kidney disease (PKD) domains, a polycystin-lipoxygenase-alphatoxin (PLAT) domain, a receptor for egg jelly (REJ) domain, and a cell-wall integrity and stress-response component (WSC). Also shown are PC1-L3040H (the PC1 GPS-cleavage mutant), PC1-ΔREJ (the REJ domain deletion mutant), PC2-R872X (a clinically relevant truncation mutant), PC2-D511V (a clinically relevant channel-dead mutant), and PC2-T721A (another channel-dead mutant). The positions of the epitope tags are indicated.

Received: February 23, 2013
Revised: June 17, 2013
Published: July 12, 2013

   dx.doi.org/10.1021/bi400233e | *Biochemistry* 2013, 52, 5280−5287

PC1 undergoes autoproteolytic cleavage at its GPS site, which is a process that appears to be required for its function.[13,14] The C-terminal tail of PC1 can also be cleaved, causing the release of fragments that enter the nucleus and regulate cell-signaling pathways.[15,16] Coexpression studies have shown that PC2 promotes both GPS cleavage of PC1 [17] and cleavage at the C-terminal tail.[18]

PC1 and PC2 can interact via C-terminal cytoplasmic coiled-coil domains[19,20] to form a polycystin complex. Exogenously expressed PC1 and PC2 have been shown to colocalize at the cell surface,[21−23] and plasma-membrane delivery of PC1 has been shown to depend on PC1 GPS cleavage.[17] In vivo, PC1 and PC2 are expressed in kidney tubular epithelial cells where they colocalize at primary cilia.[24,25] In ciliated LLC-PK$_1$ cells, colocalization of PC1 and PC2 at the cilia is promoted by PC2 channel activity and involves a coiled-coil interaction between the two proteins.[17]

Cells cultured from ADPKD cysts have lower Ca^{2+} concentrations than those from normal kidney tissue,[26] indicating that the deregulation of PC1- and PC2-mediated cellular Ca^{2+} signaling may be important in the development of the disease. PC1 has also been implicated in controling PC2 channel activity. Patch-clamp experiments showed that removal of the C-terminal coiled-coil domains from either PC1 or PC2 decreased the PC1-PC2 interaction and reduced Ca^{2+} flux.[21] Some studies have suggested that PC1 and PC2 together act as a cellular mechanosensor that is stimulated by extracellular stimuli. For example, in embryonic kidney cells expressing both PC1 and PC2, antibodies directed against the extracellular region of PC1 increased cytosolic Ca^{2+}.[23] Furthermore, the use of fluid flow to bend the primary cilium of MDCK cells caused an increase in intracellular Ca^{2+},[27] but cells lacking PC1 or incubated with antibodies directed against the extracellular regions of PC1 and PC2 showed a reduced Ca^{2+} influx.[28]

Having recently resolved the domain structure of PC1 using AFM,[10] we set out here to investigate the structural basis of the interaction between PC1 and PC2. We show that PC1 undergoes a conformational change when coexpressed with PC2. This change involves the PKD repeats and to a lesser extent the REJ domain but does not require a stable interaction between PC1 and PC2, cell surface delivery of PC1, PC2 channel function, or GPS cleavage of PC1.

MATERIALS AND METHODS

Constructs. The wild-type mouse PC1 construct, containing a triple FLAG tag near the N terminus and a triple HA tag at the C terminus,[29] together with the L3040H PC1 GPS-cleavage mutant,[30] both in pcDNA3.1, were kindly provided by Dr. M. J. Caplan (Yale University, New Haven, CT). PKD-ΔREJ (Δ2142C-2926L) was created by inserting a PCR product containing the region encoding the sixteenth PKD domain into the EcoRV and SacII restriction sites. Wild-type human PC2 as well as PC2-R872X, PC2-D511V, and PC2-T721A mutants, all tagged with V5 and His_6 at the C terminus in pcDNA3.1, were produced in-house. The constructs used are illustrated schematically in Figure 1.

Cell Culture and Transfection. tsA 201 cells were grown as described previously.[10] A total of 250 μg of DNA was used to transfect tsA 201 cells in 5 × 162 cm^2 culture flasks. For tsA 201 cells in a 75 cm^2 culture flask, 25 μg of DNA was used. After transfection, cells were incubated for 48 h to allow protein expression.

Solubilization and Isolation of Epitope-Tagged Proteins. A crude membrane fraction of transfected tsA 201 cells was solubilized in 1% Triton X-100 for 1 h before centrifugation at 100 000*g* to remove insoluble material. To isolate PC1, the solubilized extract was incubated with anti-HA-agarose beads (Sigma) for 2 h at 4 °C. The beads were washed extensively, and bound proteins were eluted with HA peptide (300 μg/mL). Eluted samples were analyzed by SDS-polyacrylamide gel electrophoresis (SDS-PAGE), and proteins were detected either by silver staining or immunoblotting.

Cell-Surface Biotinylation. Transiently transfected tsA 201 cells in one 75 cm^2 flask were washed with ice-cold phosphate-buffered saline (PBS) and incubated with 250 μM Sulfo-NHS-SS-biotin (Thermo Scientific) in PBS for 45 min at 4 °C. The reaction was quenched for 30 min at 4 °C with 300 mM NaCl and 50 mM Tris-HCl, pH 7.2. The cells were solubilized in 1% Triton X-100 for 1 h before centrifugation at 20 800*g* for 15 min. The lysates were incubated with streptavidin-agarose beads for 2 h at 4 °C, and the beads were washed thoroughly before elution in SDS-PAGE sample buffer.

AFM Imaging. Isolated proteins were diluted appropriately, and 45 μL of the sample was allowed to adsorb onto freshly cleaved, poly-L-lysine-coated mica disks. After a 5 min incubation, the sample was washed with biotechnology performance certified-grade water (Sigma) and dried in a stream of nitrogen gas. Imaging was performed with a Veeco Digital Instruments Multimode atomic force microscope controlled by a Nanoscope IIIa controller. Samples were imaged in air using tapping mode. The silicon cantilevers used had a drive frequency ~300 kHz and a specified spring constant of 40 N/m (Olympus). The applied imaging force was kept as low as possible (A_S/A_0 ~0.85).

The molecular volumes of protein particles were determined from particle dimensions on the basis of AFM images. After adsorption of the proteins onto the mica support, the particles adopted the approximate shape of a spherical cap. Scanning Probe Image Processor (SPIP) version 5 (Image Metrology) was used to measure the particle height (z_{max}) and diameter. It is well known that the geometry of the scanning AFM probe introduces a tendency to overestimate particle diameter. To minimize this probe convolution error, we used an SPIP particle threshold of 0.3 nm to provide accurate measurements of the diameter. This value was chosen after comparing the volumes calculated manually for immunoglobulin G molecules with both the volumes generated using SPIP and the predicted volume, which is based on the molecular mass. The molecular volume was calculated using the equation

$$V_m = (\pi h/6)(3r^2 + h^2) \quad (1)$$

where h is the particle height and r is the radius. The molecular volume based on the molecular mass was calculated using the equation

$$V_c = (M_0/N_0)(V_1 + dV_2) \quad (2)$$

where M_0 is the molecular mass, N_0 is Avogadro's number, V_1 and V_2 are the partial specific volumes of the particle (0.74 cm^3/g) and water (1 cm^3/g), respectively, and d is the extent of protein hydration (taken as 0.4 g of water/g of protein). Note that it has been shown previously[31] that the molecular volumes of proteins measured by imaging in air are similar to the values obtained by imaging under fluid; hence, the process of drying does not significantly affect the measured molecular volume. It

dx.doi.org/10.1021/bi400233e | Biochemistry 2013, 52, 5280−5287

has also been shown by us[32] and others[31] that there is a close correspondence between the measured and predicted molecular volumes for various proteins over a wide range of molecular masses; hence, molecular volume is measured reasonably accurately by AFM imaging.

Data Analysis. The data were separated into appropriate bin widths and histograms were plotted. Gaussian curves were fitted using SigmaPlot version 10.0, and the mean value of the peaks were calculated. Welch's *t* tests of unequal sample size and unequal variance were used to determine whether the mean particle volumes were significantly different from each other. All errors quoted are standard errors of the mean (SEM).

RESULTS

PC2 Coexpression Enhances GPS Cleavage and Cell-Surface Delivery of PC1. Wild-type PC1 was first expressed alone in tsA 201 cells and purified by immunoaffinity chromatography using its C-terminal triple HA tag. Silver staining of a purified sample revealed a band at ~460 kDa representing full-length (FL) PC1 and a fainter band at ~330 kDa corresponding to the GPS-cleaved N-terminal fragment (NTF; Figure 2A). Cleavage should generate equimolar amounts of the NTF and the C-terminal fragment (CTF), which will be isolated directly through the triple HA tag. However, the ratio of the molecular masses of the NTF and CTF is about 3:1; hence, the CTF will be more difficult to detect on the silver stain because the band intensities depend on the amount of protein present. By contrast, detection of the CTF on immunoblots will depend on the availability of the epitope tag, which will be the same, mole for mole, for the CTF as for FL PC1. Therefore, as expected, both FL PC1 and the CTF were detected on the anti-HA immunoblot (along with two smaller bands, which are likely to represent degradation products), whereas FL PC1 and the NTF were detected on the anti-FLAG blot. Inspection of the blots reveals that wild-type PC1 is about 50% cleaved when expressed alone and that the NTF and CTF remain at least partially associated, allowing the isolation of both through binding of the CTF to the immunobeads.

When wild-type PC1 was purified from cells coexpressing both PC1 and PC2, GPS cleavage was significantly enhanced, as judged by the clear detection of the CTF on the silver-stained gel and the dramatic enhancement of the CTF signal seen on the anti-HA immunoblot (Figure 2B). Interestingly, the ratios of FL PC1 to NTF on both the silver stain and the anti-FLAG immunoblot were similar to those seen for PC1 expressed alone, indicating that although cleavage was enhanced the tendency of cleaved NTF (a peripheral membrane protein) to adhere to the CTF was reduced. Coimmunopurification of PC2 with PC1 was confirmed through the appearance of a ~110 kDa band on an anti-V5 blot. Note, however, that PC2 was not detected on the silver stain, indicating a substoichiometric copurification.

The effect of the coexpression of PC1 and PC2 on the delivery of the two proteins to the cell surface was assessed by treating intact cells with a membrane-impermeant biotinylating reagent. Biotinylated proteins were captured using streptavidin-agarose, and the total and bound fractions were immunoblotted for PC1, PC2, and β-actin (as a control for cell permeabilization; Figure 2C). In agreement with the result of the previous experiment, PC2 coexpression increased GPS cleavage of PC1, as indicated by the stronger signal for total CTF on the anti-HA blots in the presence of PC2. The enhancement of the cell-surface delivery of the CTF in the presence of PC2 was even more dramatic. However, according to the anti-FLAG blot, both FL PC1 and GPS-cleaved PC1 NTF could be detected at the cell surface in similar relative amounts regardless of PC2 expression, indicating that after GPS cleavage much of the NTF dissociated from the CTF, which is again consistent with the results presented in Figure 2B. The amount of PC1 at the cell surface was not substantially affected by coexpression of PC2, indicating that almost all of the additional PC1 at the cell surface has undergone GPS cleavage. The anti-V5 blot showed that PC1 expression increased the delivery of PC2 to the cell

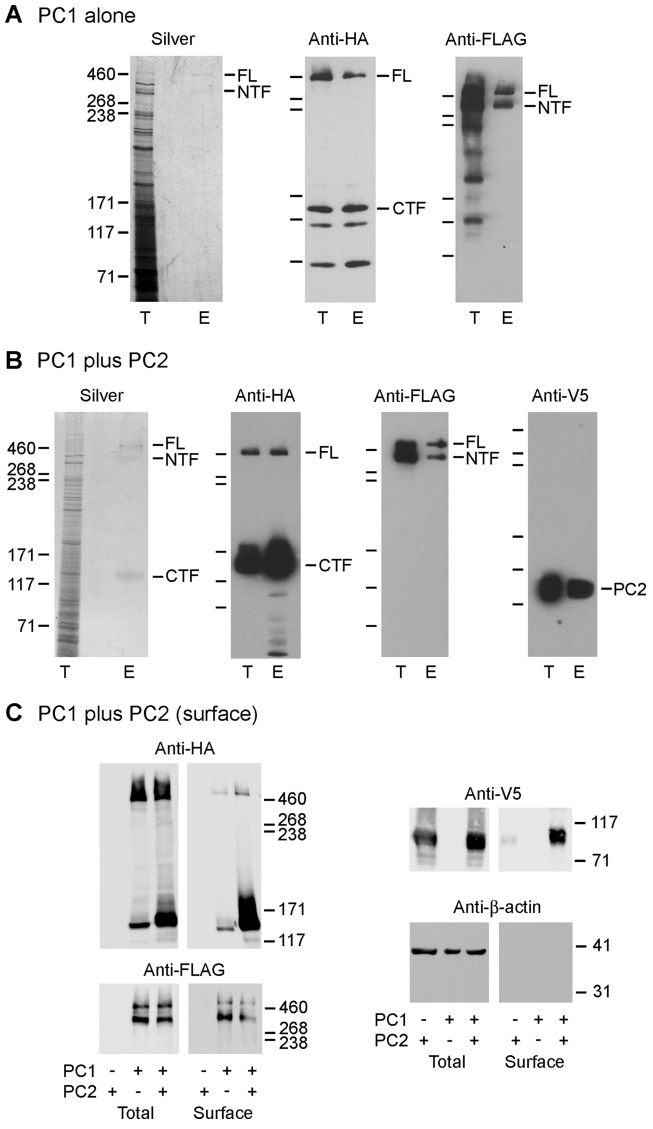

Figure 2. PC2 coexpression enhances GPS cleavage and cell-surface delivery of PC1. (A) FLAG/HA-tagged PC1 expressed alone and purified by anti-HA immunoaffinity chromatography was analyzed by either silver staining or immunoblotting with anti-HA and anti-FLAG antibodies. Total (T) and eluted (E) samples are shown. FL PC1, CTF, and NTF are indicated (right). Molecular mass markers (kDa) are shown (left). (B) FLAG/HA-tagged PC1 coexpressed with V5/His-tagged PC2 and purified by anti-HA immunoaffinity chromatography was analyzed by either silver staining or immunoblotting with anti-HA, anti-FLAG, and anti-V5 antibodies. PC1, CTF, NTF, and PC2 are indicated (right). (C) Immunoblot analysis of surface-biotinylated PC1 and PC2 expressed alone or together using anti-HA, anti-FLAG, anti-V5, and anti-β-actin antibodies.

dx.doi.org/10.1021/bi400233e | *Biochemistry* 2013, 52, 5280−5287

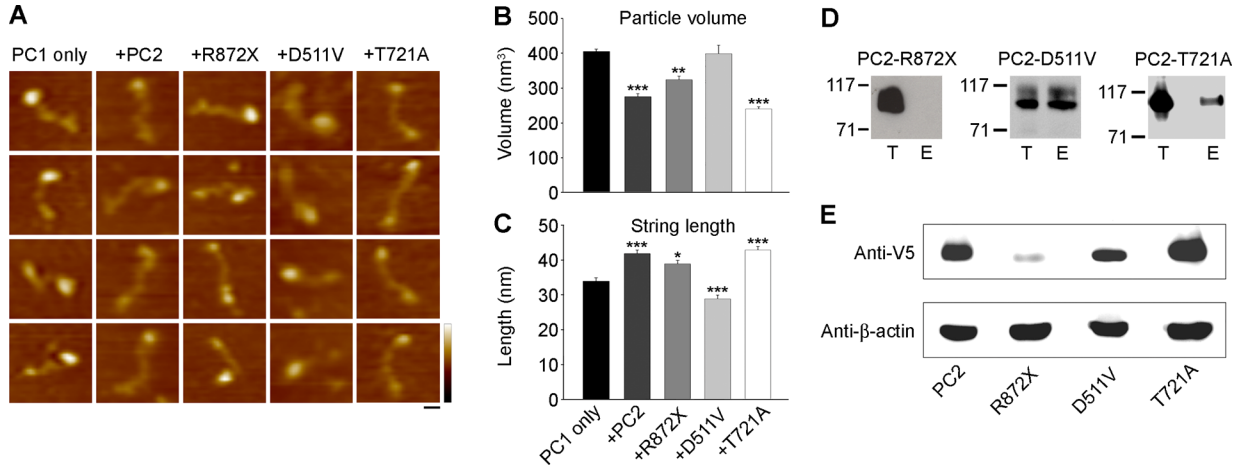

Figure 3. PC2 coexpression has a structural impact on PC1. (A) Representative AFM images of PC1 expressed alone or with PC2, PC2-R872X, PC2-D511V, and PC2-T721A. Horizontal scale bar, 20 nm; color height scale, 0–5 nm. (B) Mean volumes of large particles of PC1 when expressed alone or with PC2, PC2-R872X, PC2-D511V, and PC2-T721A. Mean volumes were calculated from Gaussian curves fitted to volume-distribution histograms. ***P < 0.001, **P < 0.01 versus PC1 alone. (C) Mean string lengths of PC1 when expressed alone or with PC2, PC2-R872X, PC2-D511V, and PC2-T721A. Mean lengths were calculated from Gaussian curves fitted to string length-distribution histograms. ***P < 0.001, *P < 0.05 versus PC1 alone. (D) FLAG/HA-tagged PC1 coexpressed with V5/His-tagged PC2-R872X, PC2-D511V, or PC2-T721A were purified by anti-HA immunoaffinity chromatography and analyzed by immunoblotting with anti-V5 antibodies. Total (T) and eluted (E) samples are shown. Molecular mass markers (kDa) are shown (left). (E) Cells were transfected with equal amounts of DNA encoding PC1 plus V5/His-tagged PC2, PC2-R872X, PC2-D511V, or PC2-T721A. Detergent extracts of crude membrane fractions were immunoblotted with anti-V5 antibodies or anti-β-actin antibodies to control for protein loading.

surface, as reported previously.[21,22] The absence of a β-actin signal in the immunoblot of the fractions bound to strepatavidin-agarose shows that intracellular proteins were not biotinylated. Note that we have reported previously[10] that when expressed in tsA 201 cells PC1 is predominantly intracellular, as indicated by immunofluorescence. Hence, even if the delivery of the protein to the cell surface is increased several fold by coexpression of PC2, only a small minority of the protein will be at the surface.

PC2 Coexpression Has a Structural Impact on PC1. AFM images of purified PC1 (Figure 3A) displayed the domain structure reported previously,[10] with FL PC1 consisting of a large C-terminal particle connected via a string of PKD domains to a smaller N-terminal particle. Given that PC2 was copurified with PC1 according to the immunoblots, we expected that the association of PC2 during coexpression would increase the mean volume of the C-terminal PC1 particle. However, AFM images showed the opposite result: in the presence of PC2 the volume of the large C-terminal particle fell by 130 nm^3 from 405 ± 7 (SEM) nm^3 (n = 197) when PC1 was expressed alone to 275 ± 8 nm^3 (n = 191) in the presence of PC2 (P < 0.001; Figure 3B). This decrease in volume was accompanied by an 8 nm increase in string length from 34 ± 1 nm (n = 197) to 42 ± 1 nm (n = 191; P < 0.001; Figure 3C). Hence, PC2 expression caused the volume of the C-terminal region of PC1 to decrease and the string length to increase, indicating an unraveling effect on PC1. The fact that the majority of the PC1 isolated during affinity chromatography is located intracellularly[10] strongly indicates that the PC2-induced conformational change in PC1 does not require delivery of the protein to the cell surface.

Stable Interaction between PC1 and PC2 Is Not Required for the Conformational Change in PC1. To determine whether a stable interaction between PC1 and PC2 was required for the conformational change in PC1, we coexpressed PC1 with PC2-R872X, which is a disease-associated truncation mutant that lacks the coiled-coil region needed for complex formation with PC1 (Figure 1; ref 19). As expected, PC2-R872X did not copurify with wild-type PC1 during the anti-HA immunoaffinity purification (Figure 3D). Nevertheless, when compared with wild-type PC1 expressed alone, the volume of the large PC1 particle decreased by 81 nm^3 to 324 ± 10 nm^3 (n = 193; P < 0.01; Figure 3A,B), and the string length increased by 5 nm to 39 ± 1 nm (n = 193; P < 0.05; Figure 3A,C). These changes were smaller than those seen with wild-type PC2, perhaps because the expression level of the PC2-R872X upon coexpression with PC1 was lower than that of the wild-type protein (Figure 3E). Nevertheless, this result demonstrates that a stable interaction between PC1 and PC2 is not required for the conformational change in PC1.

PC2 Channel Function Is Not Required for the Conformational Change in PC1. We next sought a mechanism by which PC2 may remotely alter the structure of PC1. PC2 functions as a nonselective cation channel, and a single amino acid disease-causing mutation in the third transmembrane region, D511V, is known to disrupt channel activity.[5] To test whether PC2 channel activity is required for the conformational change in PC1, PC1 and PC2-D511V were coexpressed and PC1 was captured on anti-HA immunobeads. In contrast to PC2-R872X, PC2-D511V was efficiently copurified with PC1 (Figure 3D). However, analysis of the AFM images (Figure 3A) showed that the volume of the large particle (399 ± 24 nm; n = 198) was not significantly different from that of PC1 expressed alone (Figure 3B). Interestingly, a 5 nm reduction in string length to 29 ± 1 nm (n = 198; P < 0.001) was seen (Figure 3C), suggesting that PC2-D511V might have a dominant-negative effect on the function of wild-type PC2.[12] The lack of a corresponding effect on the volume of the large particle may indicate that the tandem PKD domains tend to interact with each other as demonstrated previously[33] and that this interaction is inhibited in the presence of channel-active PC2. The behavior of the PC2-D511V mutant suggested

dx.doi.org/10.1021/bi400233e | Biochemistry 2013, 52, 5280–5287

that PC2 channel function might be required for the unraveling of PC1. To explore this possibility further, we examined the effect of another channel-dead mutant, PC2-T721A.[34] As with PC2-D511V, PC2-T721A was efficiently copurified with PC1 (Figure 3D). Note also that the expression levels of both PC2-D511V and PC2-T721A in the presence of PC1 were similar to that of wild-type PC2 (Figure 3E). Surprisingly, PC2-T721A had a similar effect on the structure of PC1 as that of wild-type PC2, reducing the volume of the large PC1 particle by 166 nm^3 to 239 ± 6 nm^3 (n = 200; P < 0.001; Figure 3A,B) and increasing the string length by 9 nm to 43 ± 1 nm (n = 200; P < 0.001; Figure 3A,C). This result indicates that PC2 channel function is not required for the conformational change in PC1; hence, the D511V mutation must have a negative effect on the function of PC2 in addition to its inhibition of channel function.

GPS Cleavage of PC1 Is Not Required for PC2-Induced Conformational Change. To test whether the conformational change in PC1 in the presence of PC2 involves GPS cleavage, we coexpressed PC2 with the PC1 GPS-cleavage mutant PC1-L3040H (Figure 1; ref 30). Silver staining and immunoblotting with both anti-HA and anti-FLAG antibodies now revealed a single major band at ~460 kDa, and the anti-V5 immunoblot showed that PC2 was copurified with PC1-L3040H (Figure 4A). When coexpressed with PC2, the mean large-particle volume of PC1-L3040H decreased by 59 nm^3 compared with PC1-L3040H alone from 429 ± 7 nm^3 (n = 198) to 370 ± 8 nm^3 (n = 187; P < 0.05; Figure 4B,C), whereas the mean string length increased by 8 nm from 28 ± 1 nm^3 (n = 198) to 36 ± 1 nm (n = 187; P < 0.001; Figure 4B,D). Hence, GPS cleavage is not required for the observed structural alterations in PC1.

REJ Domain Contributes to the Conformational Change in PC1. We have shown previously that several PKD domains and the REJ domain contribute to the volume of the large particle.[10] When PC1 is coexpressed with PC2, the REJ domain itself could become incorporated into the string or alternatively control the release of PKD domains from the large particle. To explore these possibilities, we created the construct PC1-ΔREJ that lacked amino acids C2142-L2926, which represent the REJ domain and part of the linker between the REJ domain and the GPS domain (Figure 1). PC1-ΔREJ was purified from cells coexpressing PC1-ΔREJ and PC2. A band at ~390 kDa was detected on the silver-stained gel, corresponding to full length PC1-ΔREJ (Figure 5A). The same band was also seen on anti-HA and anti-FLAG blots. Lower molecular-mass bands, which likely represent degradation products, were also seen. In contrast to the anti-HA immunoblot of wild-type PC1 (Figure 2A, B), a strong ~130 kDa CTF band was not detected with PC1-ΔREJ, demonstrating that the REJ domain is required for efficient GPS cleavage, as reported previously.[13]

AFM imaging of PC1-ΔREJ (Figure 5B) revealed that when expressed alone the mean volume of the large particle, 181 ± 12 nm^3 (n = 199; Figure 5C), was significantly (P < 0.001) smaller than that for FL PC1 not only when it was expressed alone but also when FL PC1 was expressed with PC2 (Figure 3B). Hence, when wild-type PC1 is expressed with PC2, the whole of the REJ domain cannot become incorporated into the string during the conformational change. Furthermore, because the mean string length of PC1-ΔREJ, 31 ± 0.3 nm (n = 199; Figure 5D), was not significantly different from that of FL PC1 (34 ± 1 nm; Figure 3C), the REJ domain cannot be required to secure the PKD domains to the large particle. When PC1-ΔREJ was coexpressed with PC2, the mean volume of the large particle, 133 ± 10 nm^3 (n = 200; Figure 5B,C), was not significantly affected. However, the string length, 36 ± 0.5 nm (n = 200; Figure 5B,D), was significantly increased (P < 0.001). Taken together, these results indicate that the tandem PKD domains, and probably to a lesser extent the REJ domain, both contribute to the increase in string length seen in the presence of PC2.

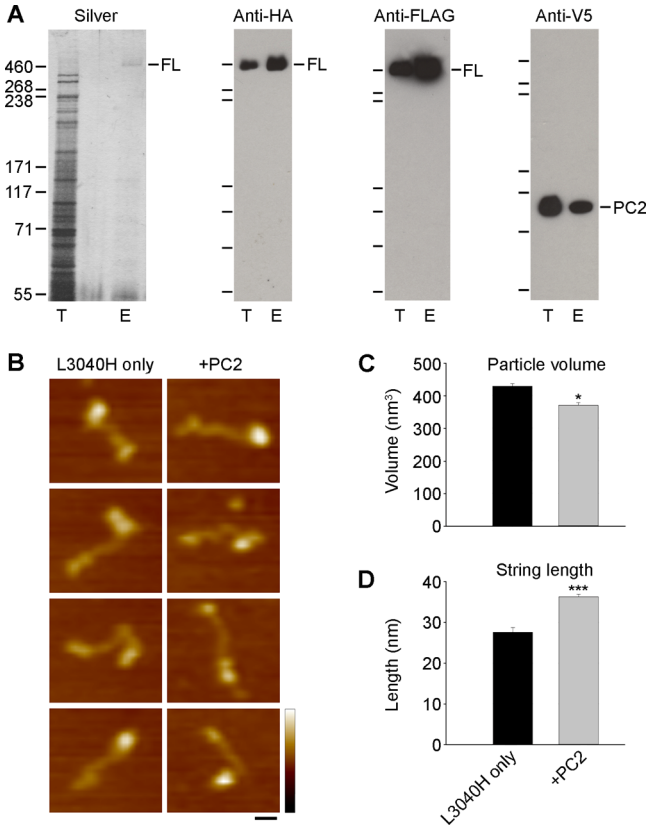

Figure 4. GPS cleavage is not required for the PC2-induced conformational change in PC1. (A) FLAG/HA-tagged PC1-L3040H and coexpressed V5/His-tagged PC2, purified by anti-HA immunoaffinity chromatography, were analyzed by either silver staining or immunoblotting with anti-HA, anti-FLAG, and anti-V5 antibodies. Total (T) and eluted (E) samples are shown. FL PC1-L3040H and PC2 are indicated (right). Molecular mass markers (kDa) are shown (left). (B) Representative AFM images of PC1-L3040H structures when expressed alone or with PC2. Horizontal scale bar, 20 nm; color height scale, 0–5 nm. (C) Mean volumes of large particles of PC1-L3040H when expressed alone or with PC2. Mean volumes were calculated from Gaussian curves fitted to volume-distribution histograms. *P < 0.05 versus PC1-L3040H alone. (D) Mean string lengths of PC1-L3040H when expressed alone or with PC2. Mean lengths were calculated from Gaussian curves fitted to string length-distribution histograms. ***P < 0.001 versus PC1-L3040H alone.

DISCUSSION

PC1 and PC2 are believed to form a Ca^{2+}-permeable ion-channel complex[21] that transduces extracellular mechanical stimuli via the renal primary cilium[28] and regulates multiple intracellular Ca^{2+}-sensitive signaling pathways.[21,23] PC2 also appears to have a role, which is independent of PC1, in regulating Ca^{2+} efflux from the ER.[35,36] It is clear that PC1 and PC2 are not always colocalized; for example, only PC2 is found in the cilia of the embryonic node,[37] and the knockout of PC2

dx.doi.org/10.1021/bi400233e | Biochemistry 2013, 52, 5280–5287

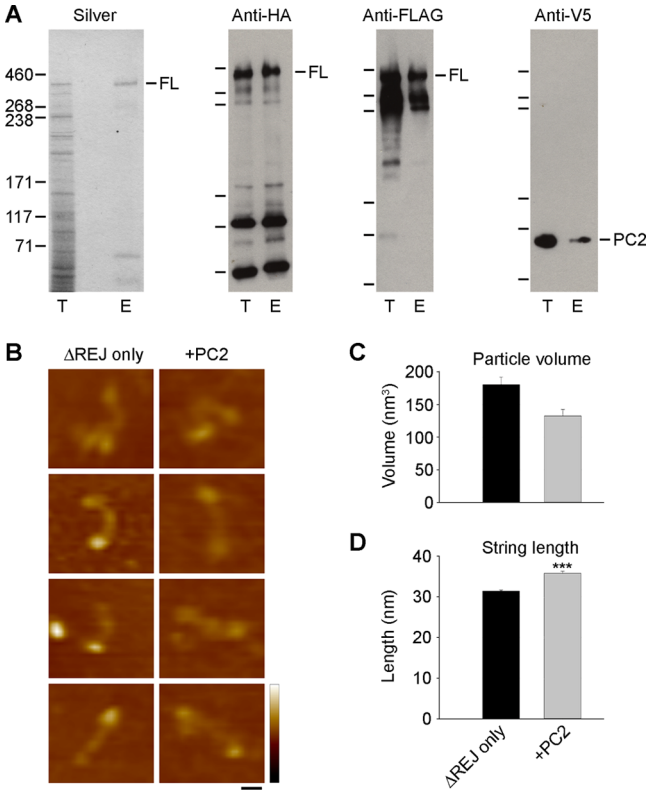

Figure 5. Removal of the PC1 REJ domain reduces the PC2-induced conformational change in PC1. (A) FLAG/HA-tagged PC1-ΔREJ and coexpressed V5/His-tagged PC2, purified by anti-HA immunoaffinity chromatography, were analyzed by either silver staining or immunoblotting with anti-HA, anti-FLAG, and anti-V5 antibodies. Total (T) and eluted (E) samples are shown. FL PC1-ΔREJ and PC2 are indicated (right). Molecular mass markers (kDa) are shown (left). (B) Representative AFM images of PC1-ΔREJ structures when expressed alone or with PC2. Horizontal scale bar, 20 nm; color height scale, 0−5 nm. (C) Mean volumes of large particles of PC1-ΔREJ when expressed alone or with PC2. Mean volumes were calculated from Gaussian curves fitted to volume-distribution histograms. (D) Mean string lengths of PC1-ΔREJ when expressed alone or with PC2. Mean lengths were calculated from Gaussian curves fitted to string length-distribution histograms. ***$P < 0.001$ versus PC1-ΔREJ alone.

causes left-right symmetry defects in mice.[38] In the present study, we have found that PC2 copurifies with PC1, but it does so substoichiometrically, suggesting a rather transient association between the two proteins. This suggestion is borne out by our failure to detect either PC2 on silver-stained gels or a PC1/PC2 complex by AFM imaging. This result is in contrast to a previous report claiming the detection of a 1:3 complex between PC1 and PC2.[39]

Although we found no evidence for a stable complex between PC1 and PC2, it was clear that the two proteins were functionally interacting within the cells; for example, PC2 enhanced GPS cleavage of PC1, and both proteins were delivered to the cell surface more efficiently when they were coexpressed, which is in agreement with previous reports.[17,21,22] Intriguingly, the presence of PC2 caused an unraveling of the structure of PC1. This effect of PC2 did not require surface delivery of PC1 and was also seen with the PC1-L3040H GPS-cleavage mutant. The conformational change in PC1 persisted when the interaction of PC2 with PC1 was abolished by a PC2-truncation mutation. Of the two channel-dead PC2 mutants tested, one, PC2-D511V, failed to cause the conformational change and indeed appeared to exert a dominant-negative effect, reducing the string length observed with PC1 alone. In contrast, the other channel-dead mutant, PC2-T721A, mimicked the effect of wild-type PC2. Our results closely parallel those of a previous study,[17] which demonstrated that in HEK293 cells PC2 increases the surface delivery of PC1 and this effect does not require either a stable interaction between PC1 and PC2 or PC2 channel activity.

The mean size of the large C-terminal particle of wild-type PC1 when coexpressed with PC2 was smaller than the corresponding particle of a PC1 mutant lacking PKD domains 6−15, as measured in our previous study,[10] but it was larger than the C-terminal particle of a mutant lacking PKD domains 5−16 and most of the REJ domain. In addition, the complete removal of the REJ domain in this study abolished the effect of PC2 on the large particle volume but not on the string length. Together, these data suggest that the PKD domains and possibly part of the REJ domain separate from the large particle and join the string structure in the presence of PC2. This rearrangement might be responsible for the observed increase in autoproteolytic GPS cleavage of PC1 in the presence of PC2 and the consequent detachment of the NTF from the CTF.[13]

Our study represents the first report of an effect of PC2 on the conformation of PC1. We propose that PC2 promotes a rearrangement of the structure of PC1, which enhances GPS cleavage and separation of the NTF from the CTF and may prepare PC1 for its functional role at the plasma membrane.

AUTHOR INFORMATION

Corresponding Author

*Phone: +44 1223 334014. Fax: +44 1223 334100. E-mail: jme1000@cam.ac.uk.

Funding

M.M.U.T. is supported by a Merit Scholarship from the Islamic Development Bank. A.P.S. is a member of the University of Cambridge MB/PhD Programme and was supported by the Jean Shanks Foundation and the James Baird Fund. This work was supported by Kidney Research U.K.

Notes

The authors declare no competing financial interest.

ACKNOWLEDGMENTS

We are very grateful to Dr. M. J. Caplan (Yale University, CT) for providing the wild-type and GPS-cleavage mutant constructs of PC1.

ABBREVIATIONS

AFM, atomic force microscopy; ADPKD, autosomal dominant polycystic kidney disease; CTF, C-terminal fragment; ER, endoplasmic reticulum; FL, full length; GPS, G protein-coupled receptor proteolytic site; HA, hemagglutinin; NTF, N-terminal fragment; PC, polycystin; PLAT, polycystin-lipoxygenase-alphatoxin; REJ, receptor for egg jelly; SPIP, scanning probe image processor; TRP, transient receptor potential; SEM, standard error of the mean; WSC, cell-wall integrity and stress-response component

REFERENCES

(1) Yoder, B. K., Mulroy, S., Eustace, H., Boucher, C., and Sandford, R. (2006) Molecular pathogenesis of autosomal dominant polycystic kidney disease. *Expert Rev. Mol. Med. 8*, 1−22.

(2) Harris, P. C., and Torres, V. E. (2009) Polycystic kidney disease. *Annu. Rev. Med. 60*, 321−337.
(3) Chapin, H. C., and Caplan, M. J. (2010) The cell biology of polycystic kidney disease. *J. Cell Biol. 191*, 701−710.
(4) González-Perrett, S., Kim, K., Ibarra, C., Damiano, A. E., Zotta, E., Batelli, M., Harris, P. C., Reisin, I. L., Arnaout, M. A., and Cantiello, H. F. (2001) Polycystin-2, the protein mutated in autosomal dominant polycystic kidney disease (ADPKD), is a Ca^{2+}-permeable nonselective cation channel. *Proc. Natl. Acad. Sci. U.S.A. 98*, 1182−1187.
(5) Koulen, P., Cai, Y., Geng, L., Maeda, Y., Nishimura, S., Witzgall, R., Ehrlich, B. E., and Somlo, S. (2002) Polycystin-2 is an intracellular calcium release channel. *Nat. Cell Biol. 4*, 191−197.
(6) Kobori, T., Smith, G. D., Sandford, R., and Edwardson, J. M. (2009) The transient receptor potential (TRP) channels TRPP2 and TRPC1 form a heterotetramer with a 2:2 stoichiometry and an alternating subunit arrangement. *J. Biol. Chem. 284*, 35507−35513.
(7) Stewart, A. P., Smith, G. D., Sandford, R., and Edwardson, J. M. (2010) Atomic force microscopy reveals the alternating subunit arrangement of the TRPP2-TRPV4 heterotetramer. *Biophys. J. 99*, 790−797.
(8) Feng, S., Okenka, G. M., Bai, C.-X., Streets, A. J., Newby, L. J., DeChant, B. T., Tsiokas, T., Obara, T., and Ong, A. C. M. (2008) Identification and functional characterization of an N-terminal oligomerization domain for polycystin-2. *J. Biol. Chem. 283*, 28471−28479.
(9) Ćelić, A. S., Petri, E. T., Benbow, J., Hodsdon, M. E., Ehrlich, B. E., and Boggon, T. J. (2012) Calcium-induced conformational changes in C-terminal tail of polycystin-2 are necessary for channel gating. *J. Biol. Chem. 287*, 17232−17240.
(10) Oatley, P., Stewart, A. P., Sandford, R., and Edwardson, J. M. (2012) Atomic force microscopy imaging reveals the domain structure of polycystin-1. *Biochemistry 51*, 2879−2888.
(11) Ruch, C., Skiniotis, G., Steinmetz, M. O., Walz, T., and Ballmer-Hofer, K. (2007) Structure of a VEGF−VEGF receptor complex determined by electron microscopy. *Nat. Struct. Mol. Biol. 14*, 249−250.
(12) Ma, R., Li, W.- P., Rundle, D., Kong, J., Akbarali, H. I., and Tsiokas, L. (2005) PKD2 functions as an epidermal growth factor-activated plasma membrane channel. *Mol. Cell. Biol. 25*, 8285−8298.
(13) Qian, F., Boletta, A., Bhunia, A. K., Xu, H., Ahrabi, A. K., Watnick, T. J., Zhou, F., and Germino, G. G. (2002) Cleavage of polycystin-1 requires the receptor for egg jelly domain and is disrupted by human autosomal-dominant polycystic kidney disease 1-associated mutations. *Proc. Natl. Acad. Sci. U.S.A. 99*, 16981−16986.
(14) Yu, S., Hackmann, K., Gao, J., He, X., Piontek, K., García González, M. A., Menezes, L. F., Xu, H., Germino, G. G., Zuo, J., and Qian, F. (2007) Essential role of cleavage of polycystin-1 at G protein-coupled receptor proteolytic site for kidney tubular structure. *Proc. Natl. Acad. Sci. U.S.A. 104*, 18688−18693.
(15) Chauvet, V., Tian, X., Husson, H., Grimm, D. H., Wang, T., Hiesenberger, T., Igarashi, P., Bennett, A. M., Ibraghimov-Beskrovnaya, O., Somlo, S., and Caplan, M. J. (2004) Mechanical stimuli induce cleavage and nuclear translocation of the polycystin-1 C terminus. *J. Clin. Invest. 114*, 1433−1443.
(16) Low, S. H., Vasanth, S., Larson, C. H., Mukherjee, S., Sharma, N., Kinter, M. T., Kane, M. E., Obara, T., and Weimbs, T. (2006) Polycystin-1, STAT6, and P100 function in a pathway that transduces ciliary mechanosensation and is activated in polycystic kidney disease. *Dev. Cell 10*, 57−69.
(17) Chapin, H. C., Rajendran, V., and Caplan, M. J. (2010) Polycystin-1 surface localization is stimulated by polycystin-2 and cleavage at the G protein-coupled receptor proteolytic site. *Mol. Biol. Cell 21*, 4338−4348.
(18) Bertuccio, C. A., Chapin, H. C., Cai, Y., Mistry, K., Chauvet, V., Somlo, S., and Caplan, M. J. (2009) Polycystin-1 C-terminal cleavage is modulated by polycystin-2 expression. *J. Biol. Chem. 284*, 21011−21026.
(19) Qian, F., Germino, F. J., Cai, Y., Zhang, X., Somlo, S., and Germino, G. G. (1997) PKD1 interacts with PKD2 through a probable coiled-coil domain. *Nat. Genet. 16*, 179−183.
(20) Tsiokas, L., Kim, E., Arnould, T., Sukhatme, V. P., and Walz, G. (1997) Homo and heterodimeric interactions between the gene products of PKD1 and PKD2. *Proc. Natl. Acad. Sci. U.S.A. 94*, 6965−6970.
(21) Hanaoka, K., Qian, F., Boletta, A., Bhunia, A. K., Piontek, K., Tsiokas, L., Sukhatme, V. P., Guggino, W. B., and Germino, G. G. (2000) Co-assembly of polycystin-1 and -2 produces unique cation-permeable currents. *Nature 408*, 990−994.
(22) Babich, V., Zeng, W.-Z., Yeh, B.-I., Ibraghimov-Beskrovnaya, O., Cai, Y., Somlo, S., and Huang, C.- L. (2004) The N-terminal extracellular domain is required for polycystin-1-dependent channel activity. *J. Biol. Chem. 279*, 25582−25589.
(23) Delmas, P., Nauli, S. M., Li, X., Coste, B., Osorio, N., Crest, M., Brown, D. A., and Zhou, J. (2004) Gating of the polycystin ion channel signaling complex in neurons and kidney cells. *FASEB J. 18*, 740−742.
(24) Pazour, G. J., San Agustin, J. T., Follit, J. A., Rosenbaum, J. L., and Witman, G. B. (2002) Polycystin-2 localizes to kidney cilia and the ciliary level is elevated in orpk mice with polycystic kidney disease. *Curr. Biol. 12*, R378−380.
(25) Yoder, B. K., Hou, X., and Guay-Woodford, L. M. (2002) The polycystic kidney disease proteins, polycystin-1, polycystin-2, polaris, and cystin, are co-localized in renal cilia. *J. Am. Soc. Nephrol. 13*, 2508−2516.
(26) Yamaguchi, T., Hempson, S. J., Reif, G. A., Hedge, A. M., and Wallace, D. P. (2006) Calcium restores a normal proliferation phenotype in human polycystic kidney disease epithelial cells. *J. Am. Soc. Nephrol. 17*, 178−187.
(27) Praetorius, H. A., and Spring, K. R. (2001) Bending the MDCK cell primary cilium increases intracellular calcium. *J. Membr. Biol. 184*, 71−79.
(28) Nauli, S. M., Alenghat, F. J., Luo, Y., Williams, E., Vassilev, P. M., Li, X., Elia, A. E. H., Lu, W., Brown, E. M., Quinn, S. J., Ingber, D. E., and Zhou, J. (2003) Polycystins 1 and 2 mediate mechanosensation in the primary cilium of kidney cells. *Nat. Genet. 33*, 129−137.
(29) Grimm, D. H., Cai, Y., Chauvet, V., Rajendran, V., Zeltner, R., Geng, L., Avner, E. D., Sweeney, W., Somlo, S., and Caplan, M. J. (2003) Polycystin-1 distribution is modulated by polycystin-2 expression in mammalian cells. *J. Biol. Chem. 278*, 36786−36793.
(30) Wei, W., Hackmann, K., Xu, H., Germino, G., and Qian, F. (2007) Characterization of cis-autoproteolysis of polycystin-1, the product of human polycystic kidney disease 1 gene. *J. Biol. Chem. 282*, 21729−21737.
(31) Schneider, S. W., Lärmer, J., Henderson, R. M., and Oberleithner, H. (1998) Molecular weights of individual proteins correlate with molecular volumes measured by atomic force microscopy. *Pflügers Arch. 435*, 362−367.
(32) Neaves, K. J., Cooper, L. P., White, J. H., Carnally, S. M., Dryden, D. T. F., Edwardson, J. M., and Henderson, R. M. (2009) Atomic force microscopy of the EcoKI type I DNA restriction enzyme bound to DNA shows enzyme dimerisation and DNA looping. *Nucleic Acids Res. 37*, 2053−2063.
(33) Ibraghimov-Beskrovnaya, O., Bukanov, N. O., Donohue, L. C., Dackowski, W. R., Klinger, K. W., and Landes, G. M. (2000) Strong homophilic interactions of the Ig-like domains of polycystin-1, the protein product of an autosomal dominant polycystic kidney disease gene, PKD1. *Hum. Mol. Genet. 9*, 1641−1649.
(34) Cai, Y., Anyatonwu, G., Okuhara, D., Lee, K.-B., Yu, Z., Onoe, T., Mei, C.-L., Qian, Q., Geng, L., Witzgall, R., Ehrlich, B. E., and Somlo, S. (2004) Calcium dependence of polycystin-2 channel activity is modulated by phosphorylation of Ser^{812}. *J. Biol. Chem. 279*, 19987−19995.
(35) Geng, L., Boehmerle, W., Maeda, Y., Okuhara, D. Y., Tian, X., Yu, Z., Choe, C.-U., Anyatonwu, G. I., Ehrlich, B. E., and Somlo, S. (2008) Syntaxin 5 regulates the endoplasmic reticulum channel-release

properties of polycystin-2. *Proc. Natl. Acad. Sci. U.S.A. 105*, 15920−15925.
(36) Wegierski, T., Steffl, D., Kopp, C., Tauber, R., Buchholz, B., Nitschke, R., Kuehn, E. W., Walz, G., and Köttgen, M. (2009) TRPP2 channels regulate apoptosis through the Ca^{2+} concentration in the endoplasmic reticulum. *EMBO J. 28*, 490−499.
(37) McGrath, J., Somlo, S., Makova, S., Tian, X., and Brueckner, M. (2003) Two populations of node monocilia initiate left-right asymmetry in the mouse. *Cell 114*, 61−73.
(38) Pennekamp, P., Karcher, C., Fischer, A., Schweickert, A., Skryabin, B., Horst, J., Blum, M., and Dworniczak, B. (2002) The ion channel polycystin-2 is required for left-right axis determination in mice. *Curr. Biol. 12*, 938−943.
(39) Yu, Y., Ulbrich, M. H., Li, M.-H., Buraei, Z., Chen, X.-Z., Ong, A. C. M., Tong, L., Isacoff, E. Y., and Yang, J. (2009) Structural and molecular basis of the assembly of the TRPP2/PKD1 complex. *Proc. Natl. Acad. Sci. U.S.A. 106*, 11558−11563.